New insights in nonlinear static stability analysis by the FEM

B. Pichler[1], **H.A. Mang**[1]

Abstract: In order to avoid a fully nonlinear analysis to obtain stability limits on nonlinear load-displacement paths, linear eigenvalue problems may be used to compute estimates of such limits. In this paper an asymptotic approach for assessment of the errors resulting from such estimates is presented. Based on the consistent linearization of the geometrically nonlinear static stability criterion – the so-called consistently linearized eigenvalue problem – higher-order estimation functions can be calculated. They are obtained from a scalar post-calculation performed after the solution of the eigenproblem. Different extensions of these higher-order estimation functions are presented. An *ab initio* criterion for the identification of the type of loss of stability (i.e., either bifurcation or limit-point buckling) is presented.

keyword: consistent linearization, asymptotic approach, higher-order estimation, imperfection sensitivity, stability

1 Introduction

Loss of stability is a frequent reason for failure of thin-walled structures. Computation of static stability limits, i.e., bifurcation or limit points, on nonlinear load-displacement paths of elastic structures, requires the use of a geometrically nonlinear theory. A powerful method for determination of such points is the Finite Element Method (FEM). One of several possible bases of the FEM is the principle of virtual displacements. With the help of this principle a system of nonlinear partial differential equations is converted into a system of nonlinear algebraic equations.

In order to avoid a fully nonlinear prebuckling analysis for the mere purpose of obtaining the stability limit, estimates of this limits, based on the solution of linear eigenvalue problems [Brendel (1979); Brendel, Ramm, Fischer, and Rammerstorfer (1981); Bushnell (1972); Gallagher and Yang (1968); Mallet and Marçal (1968)], have frequently been used. Mang and Helnwein, e.g., have suggested a consistent linearization of the mathematical formulation of the static stability condition [Helnwein (1991); Mang and Helnwein (1993, 1995a,b)]. It can be interpreted as the stability criterion for the tangents to the nonlinear load-displacement diagrams at a known state of equilibrium in the stable prebuckling domain.

Based on the results of the investigation of the asymptotic properties of the consistently linearized eigenvalue problem, alternative functions can be defined for the purpose of reducing the estimation error. Such estimation functions, obtained from scalar post-calculations, can be identified as estimation functions of higher order [Helnwein and Mang (1997)]. Depending on the chosen parameterization, the order of the estimation error is not necessarily equal for bifurcation points and snap-through points. Hence, the investigation of the asymptotic properties must be performed independently for both types of loss of stability.

Different extensions of the higher-order estimation functions can be derived. They should even further increase the reliability of estimates of stability limits, which may be obtained. Unfortunately, the order of such estimates is only defined in an asymptotic sense. Nevertheless, for many engineering structures the effect of the geometric nonlinearity in the prebuckling domain is moderate [Helnwein (1998)]. In this case, the general information from asymptotic analysis is not only relevant in the immediate vicinity of the stability limit, but in an extended part of the entire prebuckling domain.

Based on the angle between the eigenvector of the consistently linearized eigenvalue problem and the reference-load vector, an *a-priori* criterion to distinguish bifurcation modes from snap-through modes can be derived. Therefore, appropriate buckling-mode-specific estimation functions of higher order can be chosen for an initial estimation of the stability limit.

In order to obtain further insights into characteristic features of the consistently linearized eigenvalue-problem, the first derivatives of corresponding eigenvectors with respect to the load-parameter are taken into account. The load-parameter is a dimensionless factor by which the reference load is multiplied. In such a way functions can be introduced that describe the behavior of eigenvectors of the consistently linearized eigenvalue problem in the prebuckling domain. Particularly their rotations, i.e., changes of the shapes of the eigenmodes, are investigated separately.

Numerical examples show both, the potential and the limitation of the presented theoretical investigations. Accompanying eigenvalue-analyses of both, perfect and imperfect cylindrical shells, give an overview over the usefulness of the consistently linearized eigenvalue-problem, even for imperfection sensitive structures.

[1] Institute for Strength of Materials, Vienna University of Technology, Austria

2 Theoretical investigation

The basis for the presented theoretical studies is consistent linearization of the static stability criterion

$$\mathbf{K}_T(\lambda_S)\delta\mathbf{q} = \mathbf{0}, \tag{1}$$

where $\mathbf{K}_T$ is the tangent stiffness matrix evaluated at $\lambda = \lambda_S$, with λ_S representing the value of the load-parameter λ which corresponds to the buckling load, and $\delta\mathbf{q}$ is the vector of nodal degrees of freedom describing the shape of the buckling mode.

2.1 Consistent linearization of static stability criterion

Using a prime ($'$) as the symbol for the derivative with respect to the dimensionless load-parameter $\left(\frac{d}{d\lambda}\right)$, a Taylor series expansion of $\mathbf{K}_T$ in Eq. 1 at $\lambda < \lambda_S$ yields

$$[\mathbf{K}_T\big|_\lambda + (\lambda_S-\lambda)\mathbf{K}_T'\big|_\lambda + \frac{1}{2!}(\lambda_S-\lambda)^2\mathbf{K}_T''\big|_\lambda + \ldots]\,\delta\mathbf{q} = \mathbf{0}. \tag{2}$$

Truncation of this expansion after the second term yields the consistent linearization of the static stability criterion as

$$[\mathbf{K}_T\big|_\lambda + (\lambda^*-\lambda)\mathbf{K}_T'\big|_\lambda]\,\delta\mathbf{q}^* = \mathbf{0}, \tag{3}$$

which represents a linear eigenvalue problem. In general $\lambda^* \neq \lambda_S$ and $\delta\mathbf{q}^* \neq \delta\mathbf{q}$. λ^* may be viewed as an estimate of λ_S and $\delta\mathbf{q}^*$ as an approximation for $\delta\mathbf{q}$. Normalization of the eigenvector $\delta\mathbf{q}^*$ may be based on the quadratic form involving the matrix $\mathbf{K}_T'$. It is defined as

$$\delta\mathbf{q}^{*T}\mathbf{K}_T'\delta\mathbf{q}^* = \mp 1, \tag{4}$$

where the negative sign is relevant for positive eigenvalues $\lambda^* - \lambda$ and the positive sign holds for negative values of $\lambda^* - \lambda$. Characteristic features of the eigenvalue problem – Eq. 3 – are:

$$\delta\mathbf{q}_i^{*T}\mathbf{K}_T\delta\mathbf{q}_k^* = 0, \quad \forall\, i,k \quad \text{with} \quad (\lambda_i^*-\lambda) \neq (\lambda_k^*-\lambda), \tag{5}$$

and

$$\delta\mathbf{q}_i^{*T}\mathbf{K}_T'\delta\mathbf{q}_k^* = 0, \quad \forall\, i,k \quad \text{with} \quad (\lambda_i^*-\lambda) \neq (\lambda_k^*-\lambda). \tag{6}$$

Derivation of Eq. 3 with respect to λ and premultiplication of the obtained equation by $\delta\mathbf{q}^{*T}$ results in

$$\begin{aligned}&\delta\mathbf{q}^{*T}[\lambda^{*\prime}\mathbf{K}_T' + (\lambda^*-\lambda)\mathbf{K}_T'']\delta\mathbf{q}^* \quad + \\ &+\underbrace{\delta\mathbf{q}^{*T}[\mathbf{K}_T + (\lambda^*-\lambda)\mathbf{K}_T']}_{=0 \text{ see } Eq.\ 3}\delta\mathbf{q}^{*\prime} \quad = \quad 0,\end{aligned} \tag{7}$$

which yields the following expression of $\lambda^{*\prime}$:

$$\lambda^{*\prime} = -(\lambda^*-\lambda)\frac{\delta\mathbf{q}^{*T}\mathbf{K}_T''\delta\mathbf{q}^*}{\delta\mathbf{q}^{*T}\mathbf{K}_T'\delta\mathbf{q}^*}. \tag{8}$$

Specializing Eq. 8 for the stability limit of a bifurcation mode yields

$$\lim_{\lambda\to\lambda_S}\lambda^{*\prime} = -\underbrace{\lim_{\lambda\to\lambda_S}(\lambda^*-\lambda)}_{=0}\underbrace{\lim_{\lambda\to\lambda_S}\frac{\delta\mathbf{q}^{*T}\mathbf{K}_T''\delta\mathbf{q}^*}{\delta\mathbf{q}^{*T}\mathbf{K}_T'\delta\mathbf{q}^*}}_{\neq\infty} = 0. \tag{9}$$

To calculate $\lambda^{*\prime}$ for the stability limit of a snap-through mode, it is necessary to use a generalized parameterization. For limit-point problems $\lambda^{*\prime}|_{\lambda_S}$ follows as [Helnwein and Mang (1997)]

$$\lim_{\lambda\to\lambda_S}\lambda^{*\prime} = -\underbrace{\lim_{\lambda\to\lambda_S}(\lambda^*-\lambda)}_{=0}\underbrace{\lim_{\lambda\to\lambda_S}\frac{\delta\mathbf{q}^{*T}\mathbf{K}_T''\delta\mathbf{q}^*}{\delta\mathbf{q}^{*T}\mathbf{K}_T'\delta\mathbf{q}^*}}_{=\infty} = -1. \tag{10}$$

Fig. 1 shows typical λ^*-λ-diagrams for both types of loss of stability.

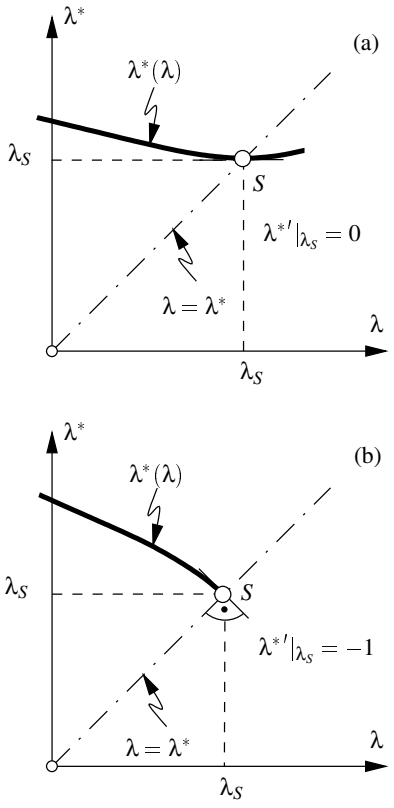

Figure 1 : Typical λ^*-λ-diagram for (a) bifurcation and (b) snap-through modes

2.2 Estimation of stability limits

2.2.1 An asymptotic approach for the evaluation of errors

To assess the quality of different estimation functions $\tilde{\lambda}^*(\lambda)$ for λ_S, an asymptotic analysis is performed: At a critical point

$(\lambda = \lambda_S)$ the error of an estimation function $\tilde{\lambda}^*(\lambda)$ of λ_S, i.e. $(\tilde{\lambda}^* - \lambda_S)$, is expressed as a Taylor series expansion

$$(\tilde{\lambda}^* - \lambda_S) = -(\lambda_S - \lambda)\,\tilde{\lambda^*}'\big|_{\lambda_S} + \frac{1}{2!}(\lambda_S - \lambda)^2\,\tilde{\lambda^*}''\big|_{\lambda_S} - -\frac{1}{3!}(\lambda_S - \lambda)^3\,\tilde{\lambda^*}'''\big|_{\lambda_S} + \ldots . \quad (11)$$

The smallest non-vanishing derivative of $\tilde{\lambda}^*(\lambda)$ with respect to λ defines the quality of this estimation function in the chosen asymptotic sense. Introducing

$$\Lambda O(n) = \left\{ \tilde{\lambda}^*(\lambda) \;\middle|\; \lim_{\lambda \to \lambda_S} \frac{d^k(\tilde{\lambda}^* - \lambda_S)}{d\lambda^k} \begin{cases} = \\ \neq \end{cases} \begin{cases} = 0 & \forall\, k \in \{0, 1, \ldots, n-1\} \\ \neq 0 & k = n \end{cases} \right\}, \quad (12)$$

a set $\Lambda O(n)$ is defined, containing estimation functions $\tilde{\lambda}^*(\lambda)$ for which the smallest non-vanishing derivative with respect to λ at a critical point is of the order n. These functions are called estimation functions of n-th order.

Asymptotic properties of estimation functions at a bifurcation-point usually differ from their behavior observed in the immediate vicinity of a snap-through point. Therefore, buckling-mode-specific subsets $\Lambda^{BIF}_{O(n)} \subset \Lambda O(n)$ and $\Lambda^{LIM}_{O(n)} \subseteq \Lambda O(n)$ for bifurcation and limit-load problems, respectively, are introduced. Assessing, e. g., the quality of $\lambda^*(\lambda)$ for modes associated with bifurcation and snap-through points, considering Eq. 9 and Eq. 10 yields

$$\lambda^* \in \Lambda^{BIF}_{O(2)} \quad \text{and} \quad \lambda^* \in \Lambda^{LIM}_{O(1)}. \quad (13)$$

2.2.2 *Higher-order estimation functions for λ_S*

Making use of the eigenvalue $\lambda^* - \lambda$ obtained from Eq. 3 and of $\lambda^{*\prime}$ according to Eq. 8 alternative estimation functions can be defined. Using an extrapolation of the estimation function λ^* at any $\lambda < \lambda_S$ along its tangent yields the estimation function $\tilde{\lambda}$ [Helnwein (1998)]. Considering the asymptotic properties of λ^* for bifurcation-buckling provides the motivation for a quadratic extrapolation for the estimation function λ^*. Forcing the slope of this parabola to be equal to zero at the estimated stability limit, results in an estimation function denoted as λ^{**} [Helnwein (1998)]. The definitions of these higher-order estimation functions are given as

$$\tilde{\lambda} = \lambda + \frac{\lambda^* - \lambda}{1 - \lambda^{*\prime}} \quad \text{and} \quad \lambda^{**} = \lambda + \frac{\lambda^* - \lambda}{1 - \frac{1}{2}\lambda^{*\prime}}. \quad (14)$$

Analysis of the asymptotic properties of the estimation functions $\tilde{\lambda}$ and λ^{**} yields [Helnwein (1998)]

$$\tilde{\lambda} \in \Lambda^{BIF}_{O(2)}, \quad \tilde{\lambda} \in \Lambda^{LIM}_{O(\underline{2})}, \quad \lambda^{**} \in \Lambda^{BIF}_{O(\underline{3})}, \quad \lambda^{**} \in \Lambda^{LIM}_{O(1)}. \quad (15)$$

To obtain a useful quadratic extrapolation for eigenvalue-curves $\lambda^*(\lambda)$ associated with a limit-point, a function of the following type can be taken:

$$\lambda^\circ(\lambda) := \lambda + \frac{\lambda^* - \lambda}{1 + x \cdot \lambda^{*\prime} + y \cdot (\lambda^{*\prime})^2}, \quad x, y \in \mathbb{R}. \quad (16)$$

The following analyses of asymptotic properties are performed in order to make a special choice for the scalar values x and y such that an estimation function of higher order is obtained. The basis for these investigations are the derivatives of $\lambda^\circ(\lambda)$ with respect to λ:

$$\lambda^{\circ\prime} = \frac{\lambda^{*\prime}(1 + x + y\lambda^{*\prime})}{1 + x\lambda^{*\prime} + y(\lambda^{*\prime})^2} - \frac{(\lambda^\circ - \lambda)\lambda^{*\prime\prime}(x + 2y\lambda^{*\prime})}{1 + x\lambda^{*\prime} + y(\lambda^{*\prime})^2}, \quad (17)$$

$$\lambda^{\circ\prime\prime} = \frac{\lambda^{*\prime\prime}(1 + 2x + 4y\lambda^{*\prime}) - 2\lambda^{\circ\prime}\lambda^{*\prime\prime}(x + 2y\lambda^{*\prime})}{1 + x\lambda^{*\prime} + y(\lambda^{*\prime})^2} - - \frac{(\lambda^\circ - \lambda)\,[\lambda^{*\prime\prime\prime}(x + 2y\lambda^{*\prime}) + 2y\lambda^{*\prime\prime 2}]}{1 + x\lambda^{*\prime} + y(\lambda^{*\prime})^2}. \quad (18)$$

To obtain an estimation function for a snap-through point, $\lambda^\circ(\lambda)$ has to be equal to λ_S at such a stability limit. From inserting Eq. 10 into Eq. 16 follows:

$$\lim_{\lambda \to \lambda_S} \lambda^\circ = \text{“}\, \lambda_S + \frac{0}{1 - x + y}\, \text{”}. \quad (19)$$

Therefore, any choice for x and y satisfying the constraint condition $1 - x + y \neq 0$ yields an estimation function for a limit-point. To obtain an estimation function of higher-order, $\lambda^{\circ\prime}(\lambda)$ has to vanish at a snap-through point. Inserting Eq. 10 into Eq. 17 considering of the limit value $\lim_{\lambda \to \lambda_S}[(\lambda^* - \lambda)\lambda^{*\prime\prime}] = 0$, [Helnwein (1998)], and forcing $1 - x + y \neq 0$, which results in $\lambda^\circ(\lambda_S) = \lambda_S$, yields

$$\lim_{\lambda \to \lambda_S} \lambda^{\circ\prime} = \text{“}\, \frac{-1 \cdot (1 + x - y)}{1 - x + y}\, \text{”} \quad (20)$$

for a snap-through point. A special choice for x and y satisfying $1 + x - y = 0$ leads to an estimation function of first order for a limit-point. Forcing $1 - x + y \neq 0$ ($\Rightarrow \lambda^\circ(\lambda_S) = \lambda_S$) and $1 + x - y = 0$ ($\Rightarrow \lambda^{\circ\prime}(\lambda_S) = 0$) the second derivative of the respective function $\lambda^\circ(\lambda)$ with respect to the load-parameter at a limit point is obtained by specializing Eq. 18 for a snap-through point as

$$\lim_{\lambda \to \lambda_S} \lambda^{\circ\prime\prime} = \text{“}\, \frac{\lambda^{*\prime\prime}|_{\lambda_S}(1 + 2x - 4y) - 2 \cdot 0 \cdot \lambda^{*\prime\prime}|_{\lambda_S}(x - 2y)}{1 - x + y} - - \frac{0 \cdot \left[\lambda^{*\prime\prime\prime}|_{\lambda_S}(x - 2y)\right] - 0 \cdot \left[2y\,(\lambda^{*\prime\prime}|_{\lambda_S})^2\right]}{1 - x + y}\, \text{”}. \quad (21)$$

To determine x and y, the equation $1 + 2x - 4y = 0$ may be chosen. This yields $x = -3/2$ and $y = -1/2$. Hence, the constraint condition $1 - x + y \neq 0$ is met. The respective function is denoted as $\tilde{\lambda}^\circ(\lambda)$. It follows as

$$\tilde{\lambda}^\circ := \lambda + \frac{\lambda^* - \lambda}{1 - \frac{3}{2}\lambda^{*\prime} - \frac{1}{2}\lambda^{*\prime 2}}. \quad (22)$$

Generally $\lambda^{*\prime\prime}(\lambda_S) = \lambda^{*\prime\prime\prime}(\lambda_S) = -\infty$ for a snap-through point. Hence, $\tilde{\lambda}^{\circ\prime\prime}(\lambda_S)$ is equal to a sum of indefinite expressions of the type $0 \cdot \infty$. In case $\lambda^{*\prime\prime}$ and $\lambda^{*\prime\prime\prime}$ are finite at a snap-through point, the curvature of $\tilde{\lambda}^{\circ}(\lambda)$ becomes zero at such a stability limit. At present, it is investigated, whether snap-through problems are existing which are characterized by a finite curvature and third-order derivative of $\lambda^*(\lambda)$ at the stability limit and, provided this is the case, what is the physical meaning of such points. In any case, what at least follows from Eq. 20 for $\tilde{\lambda}^{\circ}$ is

$$\tilde{\lambda}^{\circ} \in \Lambda^{LIM}_{O(2)}. \tag{23}$$

For the graphic interpretation of $\tilde{\lambda}^{\circ}(\lambda)$ a quadratic parabola $\hat{\lambda}^*$ can be defined as

$$\hat{\lambda}^* := \lambda^*|_{\overline{\lambda}} + (\lambda - \overline{\lambda})\,\lambda^{*\prime}|_{\overline{\lambda}} + \frac{1}{2}\beta\,(\lambda - \overline{\lambda})^2, \tag{24}$$

where β is a scalar value which must be calculated. Forcing the slope of this parabola to be equal to $\lambda^{*\prime}|_{\overline{\lambda}} \cdot (2 + \lambda^{*\prime}|_{\overline{\lambda}})$ at the estimated stability limit, i. e., $\hat{\lambda}^{*\prime}(\tilde{\lambda}^{\circ}) = \lambda^{*\prime}|_{\overline{\lambda}} \cdot (2 + \lambda^{*\prime}|_{\overline{\lambda}})$, β follows as

$$\beta = \frac{\lambda^{*\prime}|_{\overline{\lambda}} \cdot (1 + \lambda^{*\prime}|_{\overline{\lambda}})}{\tilde{\lambda}^{\circ} - \overline{\lambda}}. \tag{25}$$

The load level for which the value of the function $\hat{\lambda}^*$ is equal to its argument represents the estimated stability limit. Considering Eq. 25 a linear equation for $\tilde{\lambda}^{\circ} - \overline{\lambda}$ follows from $\hat{\lambda}^*(\tilde{\lambda}^{\circ}) = \tilde{\lambda}^{\circ}$. Solving this equation yields $\tilde{\lambda}^{\circ}(\lambda)$ according to Eq. 22.

2.2.3 *Extension of higher-order estimation functions for* λ_S

An extension of $\tilde{\lambda}$ is obtained by defining an osculating parabola $\hat{\lambda}^*(\lambda)$ for the extrapolation of λ^* at any $\lambda = \overline{\lambda}$ as

$$\hat{\lambda}^*(\lambda) = \lambda^*|_{\overline{\lambda}} + (\lambda - \overline{\lambda})\,\lambda^{*\prime}|_{\overline{\lambda}} + \frac{1}{2}(\lambda - \overline{\lambda})^2 \lambda^{*\prime\prime}|_{\overline{\lambda}}, \tag{26}$$

as shown in Figure 2. An estimation function $\tilde{\lambda}_q$ is defined by formulating the condition $\hat{\lambda}^*(\tilde{\lambda}_q) = \tilde{\lambda}_q$, which represents a quadratic equation for $(\tilde{\lambda}_q - \overline{\lambda})$. The relevant root of this equation is

$$\tilde{\lambda}_q(\lambda) = \lambda + \frac{(1 - \lambda^{*\prime})}{\lambda^{*\prime\prime}} - \frac{\sqrt{(1 - \lambda^{*\prime})^2 - 2\lambda^{*\prime\prime}(\lambda^* - \lambda)}}{\lambda^{*\prime\prime}}. \tag{27}$$

In order to obtain an extension of λ^{**}, a suitable osculating parabola of third order, $\hat{\lambda}^*(\lambda)$, can be defined for the extrapolation of λ^* at any $\lambda = \overline{\lambda}$ as

$$\begin{aligned}\hat{\lambda}^*(\lambda) \quad = \quad & \lambda^*|_{\overline{\lambda}} + (\lambda - \overline{\lambda})\,\lambda^{*\prime}|_{\overline{\lambda}} + \frac{1}{2}(\lambda - \overline{\lambda})^2 \lambda^{*\prime\prime}|_{\overline{\lambda}} + \\ & + \frac{1}{3}(\lambda - \overline{\lambda})^3 \gamma,\end{aligned} \tag{28}$$

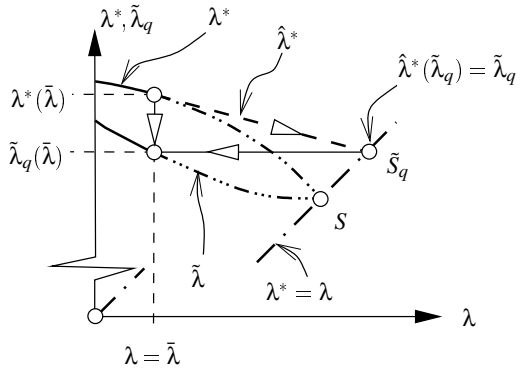

Figure 2 : Graphic interpretation of the estimation function $\tilde{\lambda}_q$

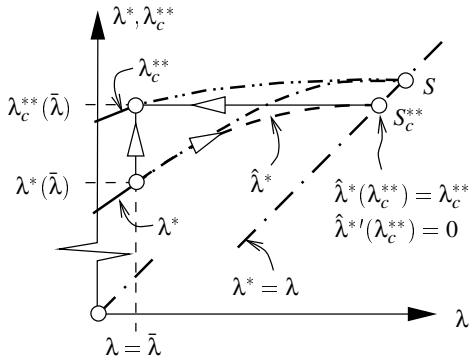

Figure 3 : Graphic interpretation of the estimation function λ_c^{**}

where γ is a coefficient which needs to be calculated. A graphic interpretation of this type of extrapolation is given in Fig. 3. Forcing the slope of $\hat{\lambda}^*$ to be zero at the estimated stability limit,

$$\hat{\lambda}^{*\prime}(\lambda_c^{**}) = \lambda^{*\prime}|_{\overline{\lambda}} + (\lambda_c^{**} - \overline{\lambda})\,\lambda^{*\prime\prime}|_{\overline{\lambda}} + (\lambda_c^{**} - \overline{\lambda})^2 \gamma = 0, \tag{29}$$

yields the following expression for γ:

$$\gamma = -\left[\frac{\lambda^{*\prime}|_{\overline{\lambda}}}{(\lambda_c^{**} - \overline{\lambda})^2} + \frac{\lambda^{*\prime\prime}|_{\overline{\lambda}}}{(\lambda_c^{**} - \overline{\lambda})}\right]. \tag{30}$$

An estimation function λ_c^{**} is defined by formulating the condition $\hat{\lambda}^*(\lambda_c^{**}) = \lambda_c^{**}$. Considering Eq. 30 this gives a quadratic equation for $(\lambda_c^{**} - \overline{\lambda})$. The relevant solution is obtained as

$$\lambda_c^{**}(\lambda) = \lambda + \frac{(3 - 2\lambda^{*\prime})}{\lambda^{*\prime\prime}} - \frac{\sqrt{(3 - 2\lambda^{*\prime})^2 - 6\lambda^{*\prime\prime}(\lambda^* - \lambda)}}{\lambda^{*\prime\prime}}. \tag{31}$$

In order to obtain an alternative extension of λ^{**} the static stability criterion – Eq. 1 – can be expressed as the product of

Taylor series expansions of $\mathbf{K}_T$ and $\delta\mathbf{q}^*$ at any $\lambda = \overline{\lambda}$ as

$$[\mathbf{K}_T + (\lambda_S - \overline{\lambda})\,\mathbf{K}_T^{\prime} + \frac{1}{2!}(\lambda_S - \overline{\lambda})^2\,\mathbf{K}_T^{\prime\prime} + \ldots] \cdot \cdot\{\delta\mathbf{q}^* + (\lambda_S - \overline{\lambda})\,\delta\mathbf{q}^{*\prime} + \ldots\} = \mathbf{0}\,. \tag{32}$$

Considering only terms containing $(\lambda_S - \overline{\lambda})^j,\ j \in \{0,1\}$, in Eq. 32 and using Eq. 38, Eq. 6, Eq. 8, and Eq. 4 yields an estimation function equivalent to λ^{**} [Pichler (1999)]. Considering terms containing $(\lambda_S - \overline{\lambda})^j,\ j \in \{0,1,2\}$, in Eq. 32 which obviously is an extension of λ^{**}, gives

$$\begin{aligned}\mathbf{K}_T\{\delta\mathbf{q}^* + (\lambda^{\diamond\diamond} - \overline{\lambda})\,\delta\mathbf{q}^{*\prime} + \tfrac{1}{2}(\lambda^{\diamond\diamond} - \overline{\lambda})^2\,\delta\mathbf{q}^{*\prime\prime}\} + \\ + (\lambda^{\diamond\diamond} - \overline{\lambda})\mathbf{K}_T^{\prime}\{\delta\mathbf{q}^* + (\lambda^{\diamond\diamond} - \overline{\lambda})\,\delta\mathbf{q}^{*\prime}\} + \\ + \tfrac{1}{2}(\lambda^{\diamond\diamond} - \overline{\lambda})^2\mathbf{K}_T^{\prime\prime}\{\delta\mathbf{q}^*\} = \mathbf{0}\,,\end{aligned} \tag{33}$$

where $\lambda^{\diamond\diamond}$ is a estimation function for λ_S. It is obtained by a consistent quadratic approximation of the static stability criterion based on $\delta\mathbf{q}^*$ and its derivatives. Premultiplying Eq. 33 by ${\delta\mathbf{q}^*}^T$ and considering Eq. 38, Eq. 6, Eq. 8, the normalization-condition – Eq. 4 –, and its derivative results in the following expression for $\lambda^{\diamond\diamond}$:

$$\lambda^{\diamond\diamond}(\lambda) = \lambda + \frac{(1 - \frac{1}{2}\lambda^{*\prime})}{{\delta\mathbf{q}^*}^T\mathbf{K}_T\delta\mathbf{q}^{*\prime\prime}} - \frac{\sqrt{(1 - \frac{1}{2}\lambda^{*\prime})^2 - 2(\lambda^* - \lambda){\delta\mathbf{q}^*}^T\mathbf{K}_T\delta\mathbf{q}^{*\prime\prime}}}{{\delta\mathbf{q}^*}^T\mathbf{K}_T\delta\mathbf{q}^{*\prime\prime}}\,. \tag{34}$$

For the computation of the estimation functions $\tilde{\lambda}_q$, λ_c^{**} and $\lambda^{\diamond\diamond}$ the second derivative of the eigenvalue-curve, $\lambda^{*\prime\prime}$, and the bilinear-form ${\delta\mathbf{q}^*}^T\mathbf{K}_T\delta\mathbf{q}^{*\prime\prime}$ can be approximated by finite difference expressions [Pichler (1999)].

2.2.4 A-priori *condition for "bifurcation modes"*

The differential form of the equilibrium condition for a solid discretized by the FEM and subjected to proportional loading is given as

$$\mathbf{K}_T d\mathbf{q} = d\lambda\overline{\mathbf{P}}. \tag{35}$$

Premultiplying Eq. 35 by the transpose of the eigenvector, $\delta\mathbf{q}^T$, and using the static stability criterion Eq. 1 yields

$$\delta\mathbf{q}^T\mathbf{K}_T d\mathbf{q}\big|_{\lambda=\lambda_S} = d\lambda\delta\mathbf{q}^T\overline{\mathbf{P}} = \mathbf{0}\,. \tag{36}$$

Equation Eq. 36 can be satisfied as shown in Tab. 1. Incidentally, a bifurcation point and a limit point may coincide. Recently it was shown, that ${\delta\mathbf{q}^*}^T\overline{\mathbf{P}} = 0$ for a bifurcation mode does not only hold at the stability limit but in the entire prebuckling domain [Mang and Helnwein (1999)].

Since the vectors $\delta\mathbf{q}^*$ and $\overline{\mathbf{P}}$ belong to $\mathbb{R}^N$, where N denotes the number of degrees of freedom, a unique angle α^* can be defined as

Table 1 : Two types of solutions of equation Eq. 36

$d\lambda \neq 0,\ {\delta\mathbf{q}^*}^T\overline{\mathbf{P}} = 0$	The eigenvector $\delta\mathbf{q}$ is orthogonal to the reference load vector $\overline{\mathbf{P}}$. This is the situation for a bifurcation point.
$d\lambda = 0,\ {\delta\mathbf{q}^*}^T\overline{\mathbf{P}} \neq 0$	The load rate becomes zero. This is the situation of a load-related limit point.

$$\cos\left(\frac{\pi}{2} - \alpha^*\right) = \frac{{\delta\mathbf{q}^*}^T\overline{\mathbf{P}}}{\sqrt{{\delta\mathbf{q}^*}^T\delta\mathbf{q}^*}\sqrt{\overline{\mathbf{P}}^T\overline{\mathbf{P}}}} \quad \Rightarrow$$
$$\Rightarrow \quad \alpha^* = \arcsin\frac{{\delta\mathbf{q}^*}^T\overline{\mathbf{P}}}{\sqrt{{\delta\mathbf{q}^*}^T\delta\mathbf{q}^*}\sqrt{\overline{\mathbf{P}}^T\overline{\mathbf{P}}}}. \tag{37}$$

The angle α^* according to Eq. 37 may be interpreted as the deviation of the eigenvector $\delta\mathbf{q}^*$ from a vector which is perpendicular to $\overline{\mathbf{P}}$. Based on Eq. 37 an alternative criterion for the identification of the type of loss of stability can be formulated as shown in Tab. 2:

Table 2 : Criterion for the identification of the type of loss of stability

$\alpha^* = 0$	the related eigenvector is corresponding to a bifurcation-mode,
$\alpha^* \neq 0$	the related eigenvector is corresponding to a snap-through-mode.

2.3 *Behavior of* $\delta\mathbf{q}^*$ *in the prebuckling domain*

In order to investigate the behavior of $\delta\mathbf{q}^*$, its first derivative with respect to the load-parameter, $\delta\mathbf{q}^{*\prime}$, has to be studied.

2.3.1 *Derivation of* $\delta\mathbf{q}^*$ *with respect to the load-parameter*

Since the eigenvectors $\delta\mathbf{q}_i^*,\ i \in \{1,2,\ldots,N\}$, form a complete basis in $\mathbb{R}^N$, $\delta\mathbf{q}_i^{*\prime}$ can be expressed as

$$\delta\mathbf{q}_i^{*\prime} = \sum_{k=1}^{N}\alpha_{ik}\,\delta\mathbf{q}_k^*\,. \tag{38}$$

Based on the normalization-condition – Eq. 4 – the coefficients $\alpha_{ik},\ i,k \in \{1,2,\ldots,N\}$, are given as [Helnwein (1998)]

$$\begin{aligned}\alpha_{ii} &= -\frac{1}{2}\frac{{\delta\mathbf{q}_i^*}^T\mathbf{K}_T^{\prime\prime}\delta\mathbf{q}_i^*}{{\delta\mathbf{q}_i^*}^T\mathbf{K}_T^{\prime}\delta\mathbf{q}_i^*} = \frac{1}{2}\frac{\lambda_i^{*\prime}}{\lambda_i^* - \lambda}, \\ \alpha_{ik} &= \frac{(\lambda_i^* - \lambda)}{(\lambda_k^* - \lambda_i^*)}\frac{{\delta\mathbf{q}_i^*}^T\mathbf{K}_T^{\prime\prime}\delta\mathbf{q}_k^*}{{\delta\mathbf{q}_k^*}^T\mathbf{K}_T^{\prime}\delta\mathbf{q}_k^*}, \quad \lambda_i^* \neq \lambda_k^*.\end{aligned} \tag{39}$$

These equations are the basis for theoretical analysis of the behavior of an eigenvector.

At an extreme value of λ_i^* in the prebuckling domain ($\lambda_i^{*\prime} = 0$), the coefficient α_{ii} becomes equal to zero. The eigenvector $\delta\mathbf{q}_i^*$ does not contribute to its own change of length at such a point. However, generally $\delta\mathbf{q}_i^*$ and $\delta\mathbf{q}_i^{*\prime}$ are not perpendicular at a point characterized by $\lambda_i^{*\prime} = 0$, since the eigenvectors $\delta\mathbf{q}_j^*$ $j \in \{1,2,\ldots,N\}$ form a oblique-angled basis in $\mathbb{R}^N$

Calculating the limit values $\lambda \rightarrow \lambda_S$ of the coefficients α_{ik}, $i,k \in \{1,2,\ldots,N\}$, where λ_S denotes the critical load-parameter for a bifurcation point, yields

$$\lim_{\lambda\to\lambda_S} \alpha_{ii} = \frac{1}{2}\lim_{\lambda\to\lambda_S}\frac{\lambda_i^{*\prime\prime}}{\lambda_i^{*\prime}-1} = -\frac{1}{2}\lambda_i^{*\prime\prime}|_{\lambda_S}, \tag{40}$$

$$\lim_{\lambda\to\lambda_S} \alpha_{ik} = \text{“}\ \frac{0}{(\lambda_k^*-\lambda)}\frac{\delta\mathbf{q}_i^{*T}\mathbf{K}_T''\delta\mathbf{q}_k^*}{\mp 1}\ \text{”} = 0,\ i \neq k. \tag{41}$$

In Eq. 40 *de L'Hospital's* rule has been used. Since α_{ii} is the only coefficient in Eq. 38 that does not vanish at a bifurcation point, $\delta\mathbf{q}_i^*$ and $\delta\mathbf{q}_i^{*\prime}$ become collinear at such a critical point. The curvature of $\lambda^*(\lambda_S)$ is a measure of the change of length of the related eigenvector at the bifurcation point.

For a snap-through mode $\delta\mathbf{q}_i^*$ the limit $\lambda \rightarrow \lambda_S$ for the coefficient α_{ii} follows as

$$\lim_{\lambda\to\lambda_S} \alpha_{ii} = \frac{1}{2}\text{“}\ \frac{-1}{0}\ \text{”} = -\infty. \tag{42}$$

Because of the

$$\lim_{\lambda\to\lambda_S} \mathbf{K}_T' = \pm\infty \qquad \text{and} \qquad \lim_{\lambda\to\lambda_S} \mathbf{K}_T'' = \pm\infty \tag{43}$$

for a snap-through point and because of the introduced normalization condition, the Euclidian norm of an eigenvector corresponding to such a point, $\delta\mathbf{q}_i^*$, must tend to zero.

For the numerical computation of $\delta\mathbf{q}^{*\prime}$, an iterative calculation scheme was developed, which requires only few iteration-steps. It was published in [Helnwein, Mang, and Pichler (1999)].

2.3.2 *Rotations and change of length of* $\delta\mathbf{q}^*$

To characterize the behavior of $\delta\mathbf{q}^*$ in the prebuckling domain, a function $\Omega(\lambda)$ is introduced which represents the cosine of the angle between $\delta\mathbf{q}^*$ and its derivative $\delta\mathbf{q}^{*\prime}$:

$$\Omega = \frac{\delta\mathbf{q}^{*\prime T}\delta\mathbf{q}^*}{\|\delta\mathbf{q}^{*\prime}\|\,\|\delta\mathbf{q}^*\|}. \tag{44}$$

At a bifurcation-point $\Omega = \pm 1$, where the positive sign holds for a negative value of the curvature of λ^* and the negative sign for $\lambda^{*\prime\prime}(\lambda_S) > 0$. At a snap-through point $\Omega = -1$. A point where $\delta\mathbf{q}^{*\prime}$ is perpendicular to $\delta\mathbf{q}^*$ is characterized by $\Omega = 0$.

$\delta\mathbf{q}^{*\prime}$ describes the change of the eigenvector $\delta\mathbf{q}^*$. It consists of both, changes of length and rotations. Therefore, $\delta\mathbf{q}^{*\prime}$ may be split into these two parts:

$$\delta\mathbf{q}^{*\prime} = \mathbf{s} + \mathbf{r}, \tag{45}$$

where $\mathbf{s}$ denotes the length-changing part and $\mathbf{r}$ stands for the rotational part of $\delta\mathbf{q}^{*\prime}$. The Euclidian norms of $\mathbf{s}$ and $\mathbf{r}$ are given as

$$\begin{aligned} \|\mathbf{s}\| &= \frac{\delta\mathbf{q}^{*\prime T}\delta\mathbf{q}^*}{\sqrt{\delta\mathbf{q}^{*T}\delta\mathbf{q}^*}}, \\ \|\mathbf{r}\| &= \sqrt{\delta\mathbf{q}^{*\prime T}\delta\mathbf{q}^{*\prime} - \frac{(\delta\mathbf{q}^{*\prime T}\delta\mathbf{q}^*)^2}{\delta\mathbf{q}^{*T}\delta\mathbf{q}^*}}. \end{aligned} \tag{46}$$

Geometrically, the eigenvectors $\delta\mathbf{q}^*$ can be viewed as moving along a one-parametric curve in $\mathbb{R}^N$, which can be plotted in an evolved manner, as shown in Figure 4. For this purpose it

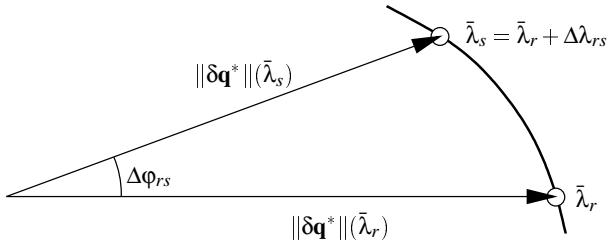

Figure 4 : Two-dimensional representation of the unwinded curve of $\delta\mathbf{q}^*$

is necessary to calculate the angular velocity of $\delta\mathbf{q}^*$. At any $\lambda = \bar{\lambda}$ it is defined as

$$\varphi' = \frac{\|\mathbf{r}(\bar{\lambda})\|}{\|\delta\mathbf{q}^*(\bar{\lambda})\|} = \sqrt{\frac{\delta\mathbf{q}_i^{*\prime T}\delta\mathbf{q}_i^{*\prime}}{\delta\mathbf{q}_i^{*T}\delta\mathbf{q}_i^*} - \left(\frac{\delta\mathbf{q}_i^{*\prime T}\delta\mathbf{q}_i^*}{\delta\mathbf{q}_i^{*T}\delta\mathbf{q}_i^*}\right)^2}. \tag{47}$$

The angular change of $\delta\mathbf{q}^*$ within an incremental loading-step from a load level $\bar{\lambda}_r$ to $\bar{\lambda}_s = \bar{\lambda}_r + \Delta\lambda_{rs}$ can be calculated by a numerical integration of Eq. 47 as

$$\Delta\varphi_{rs} \approx \frac{\Delta\lambda_{rs}}{2}\left(\frac{\|\mathbf{r}(\bar{\lambda}_r)\|}{\|\delta\mathbf{q}^*(\bar{\lambda}_r)\|} + \frac{\|\mathbf{r}(\bar{\lambda}_s)\|}{\|\delta\mathbf{q}^*(\bar{\lambda}_s)\|}\right). \tag{48}$$

3 Numerical investigation – shallow cylindrical shell

Four examples will show the relevance of the presented theoretical investigation. All examples are shallow cylindrical shells subjected to a concentrated load, as shown in Fig. 5.

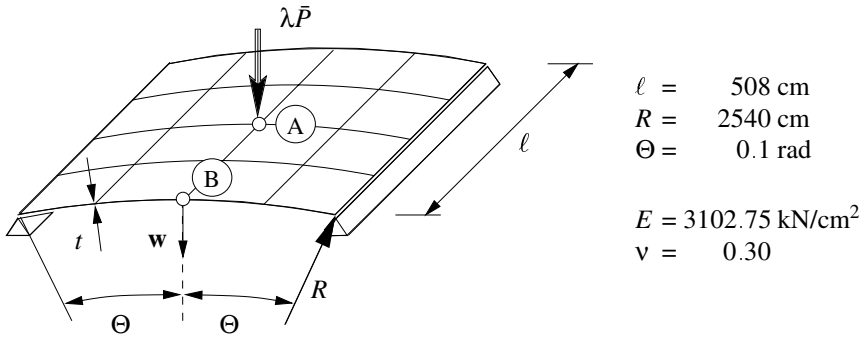

Figure 5 : Shallow cylindrical shell [Sabir and Lock (1972)]

3.1 Analysis of perfect shells

The first example is characterized by $t = 12.7$cm and $\overline{P} = 221.75$kN. For the second example $t = 6.35$cm and $\overline{P} = 52.65$kN were chosen. Because of these special choices for $\overline{P}$, the critical load-parameter is equal to 10.0 for both examples. Fig. 6 shows the load displacement curves for two points in Fig. 5, denoted as Ⓐ and Ⓑ, for both examples. The stability

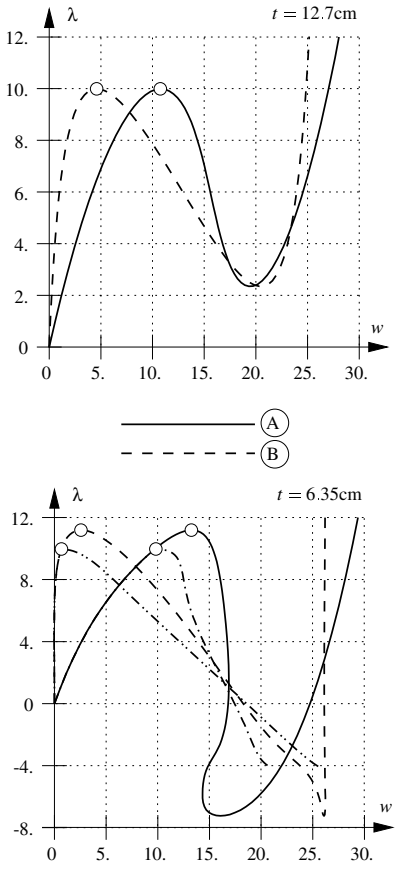

Figure 6 : Vertical deflection of Ⓐ and Ⓑ for both examples

limit of the thicker shell is a snap-through point. Theoretically, loss of stability of the thinner shell is by bifurcation buckling. However, because of the imperfection-sensitivity of this structure, it will actually lose its stability by snap-through at a load intensity which is smaller than the one corresponding to the bifurcation point. Results of respective analyses are given in subsection 3.2.

3.1.1 Estimation of stability limits

Tab. 3 contains the results from initial eigenvalue analysis as well as the angle between the corresponding eigenvectors and the reference-load vector for the three smallest positive eigenvalues for both examples. The smallest eigenvalue of the thicker shell corresponds to a snap-through mode, because $\alpha_1^* \neq 0$. Up to the computed number of digits, α_2^* and α_3^* are equal to zero. Therefore, the second and the third smallest eigenvalue correspond to bifurcation modes.

Snap-through and bifurcation modes of the thinner shell are identified in a similar manner. The smallest and the third smallest eigenvalue are associated with bifurcation modes. The second smallest eigenvalue is obviously corresponding to a snap-through mode.

The percent-wise discrepancies of the computed estimation functions at $\lambda = 0$ from λ_S for both examples are shown in Tab. 4. Results of the presented estimation functions for both examples obtained by an accompanying eigenvalue analysis for the smallest eigenvalue are shown in Fig. 7. For the thicker shell (snap-through), λ^* initially yields an overestimation of λ_S by 45.4%. Especially estimates of λ_S based on $\tilde{\lambda}^\circ$ and $\tilde{\lambda}_q$

Table 3 : Values for the angle α^* evaluated at $\lambda = 0$ for the three smallest positive eigenvalues for both examples

	$t = 12.7$cm		$t = 6.35$cm	
mode	λ^*	$\alpha^*[^\circ]$	λ^*	$\alpha^*[^\circ]$
mode 1	14.54	5.62627	8.80	0.00000
mode 2	18.80	0.00000	9.11	9.04984
mode 3	21.88	0.00000	15.33	0.00000

Table 4 : Initial discrepancies of the presented estimation functions from λ_S for both examples

$\lambda = 0$	λ^*	$\tilde{\lambda}$	$\tilde{\lambda}_q$	$\tilde{\lambda}^\circ$
$t = 12.7$cm	45.4 %	11.8 %	3.6 %	3.5 %
$t = 6.35$cm	-11.9 %	-14.3 %	- 5.6 %	-15.4 %
$\lambda = 0$	λ^*	λ^{**}	λ_c^{**}	$\lambda^{\diamond\diamond}$
$t = 12.7$cm	45.4 %	26.4 %	17.3 %	4.7 %
$t = 6.35$cm	-11.9 %	-13.1 %	-10.9 %	-14.2 %

reduce the error of λ^* for about one order of magnitude in the entire prebuckling domain. In the vicinity of the stability limit $\tilde{\lambda}^\circ$, $\tilde{\lambda}_q$ and $\tilde{\lambda}$ give the best estimates for λ_S. For the thinner shell (bifurcation), λ_S is initially underestimated by λ^* by 11.9%. At $\lambda = 0$ only $\tilde{\lambda}_q$ and λ_c^{**} provide better estimates for the stability limit. In the vicinity of λ_S the best estimates for the stability limit are obtained by means of λ_c^{**} and $\lambda^{\diamond\diamond}$. In this region of the prebuckling domain λ_c^{**} and $\lambda^{\diamond\diamond}$ result in improvements of the estimation quality of one order of magnitude as compared to estimates based on λ^*.

Because of the definition of $\tilde{\lambda}_q$, λ_c^{**}, and $\lambda^{\diamond\diamond}$ and of their observed asymptotic properties, it would seem that

$$\tilde{\lambda}_q \in \Lambda^{LIM}_{O(3)}, \quad \lambda_c^{**} \in \Lambda^{BIF}_{O(4)}, \quad \lambda^{\diamond\diamond} \in \Lambda^{BIF}_{O(4)}. \tag{49}$$

However, so far this was not proved mathematically.

3.1.2 Behavior of eigenvectors in the prebuckling domain

As shown in Fig. 8, for both examples a point exists, for which $\Omega = 0$ in the prebuckling domain. At these points $\delta\mathbf{q}^{*\prime}$ causes only qualitative changes of the shape of the eigenmode $\delta\mathbf{q}^*$, whereas its Euclidian norm does not change locally. This fact indicates the strong influence of nonlinearities of both examples, since $\delta\mathbf{q}^*$ and $\delta\mathbf{q}^{*\prime}$ become collinear at the stability limit. At the critical points, Ω tends to ± 1, i.e. $\delta\mathbf{q}^{*\prime}$ causes only quantitative changes of the shape of $\delta\mathbf{q}^*$. The quality of the shape of the eigenmode does not change at the respective stability limit.

Evolved curves of the viewed eigenvectors in $\mathbb{R}^N$ are given in Fig. 9. The eigenvector associated with the snap-through point shows a significant rotation in the prebuckling domain. The total change of direction amounts to approximate 15.5°. In contrast to this behavior, the rotation of the eigenvector associated with the bifurcation point in the entire prebuckling domain does not exceed 3.6°.

Fig. 13 to 18 show the components of $\delta\mathbf{q}^*$ and $\delta\mathbf{q}^{*\prime}$ in the vertical direction for $\lambda = 0$, at $\Omega = 0$, and at a point in the immediate vicinity of the respective stability limit.

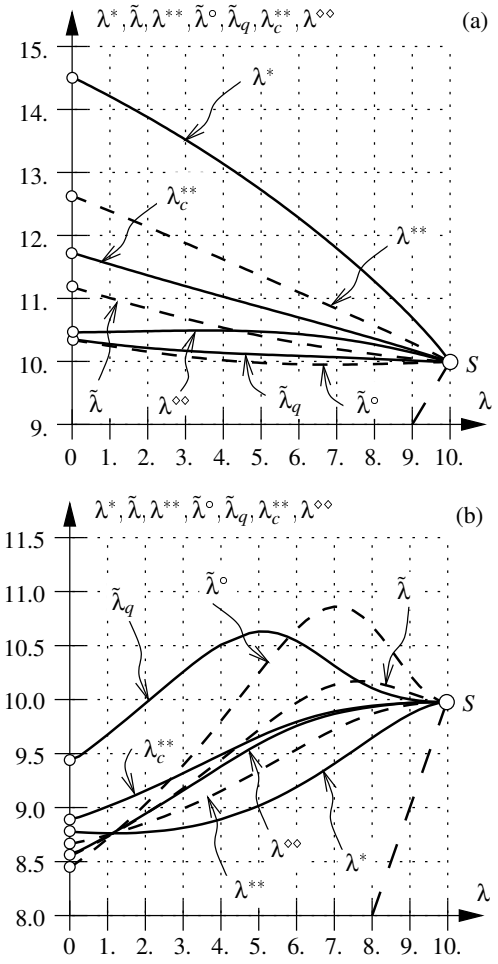

Figure 7 : λ^*-λ-diagram and higher-order estimation functions for the smallest eigenvalue for (a) example 1, $t = 12.7$cm and (b) example 2, $t = 6.35$cm ($\circ$ ... *ab initio* estimation)

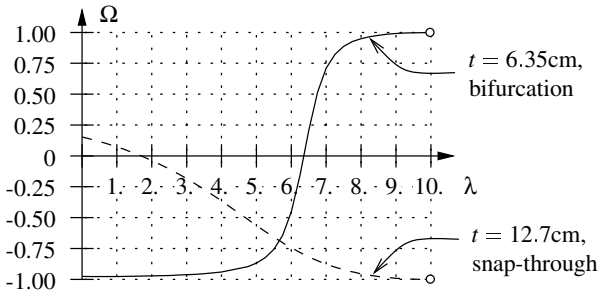

Figure 8 : Cosine between $\delta\mathbf{q}^*$ and $\delta\mathbf{q}^{*\prime}$ over the load-parameter for both examples

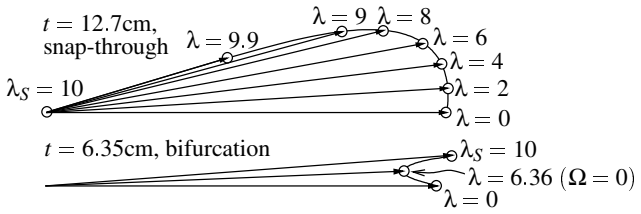

Figure 9 : Evolved curves of $\delta\mathbf{q}^*$ for both examples

3.2 *Analysis of imperfect shells*

The investigated thinner perfect shell theoretically loses its stability by bifurcation buckling. The behavior of this shell is imperfection-sensitive. Therefore, analyses of imperfect shells with $t = 6.35$cm are performed. As shown in Fig. 10, sinusoidal geometric imperfections, affine to the relevant eigenmode, were applied to the perfect structure. In order to

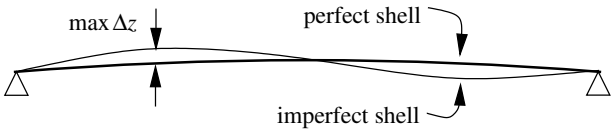

Figure 10 : Type of applied imperfections

obtain a characteristic measure for the intensity of the applied imperfection, a dimensionless imperfection-factor $\mu = (\max \Delta z / 6.35\text{cm})$ is introduced.

Fig. 11 shows eigenvalue-curves as well as load-displacement diagrams for point Ⓐ of the perfect shell ($\mu = 0\%$), and of two imperfect shells ($\mu = 2\%, \mu = 10\%$). The eigenvalue-curves obtained by accompanying eigenvalue-analyses for both imperfect structures do not differ qualitatively a lot from the eigenvalue curve for the perfect shell. However, the relevant eigenmodes of the imperfect structures are identified *ab initio*, by means of the angle α^*, as snap-through modes. Tab. 5 shows the values of α^* for the relevant eigenmodes of both imperfect structures, at $\lambda = 0$. The slope of both eigenvalue-

Table 5 : Initial values of α^* for the relevant eigenmodes

$\lambda = 0$	$\mu = 2\%$	$\mu = 10\%$
α^*	$3.293°$	$4.821°$

curves is equal to -1 at the snap-through point. Hence, the amount of $\lambda^{*\prime\prime}$ increases rapidly in the immediate vicinity of the related stability limits. Moreover, the associated asymptotic domains are restricted to the immediate vicinity of the snap-through points.

In order to assess the reliability of initial estimates as a function of the applied imperfection, the initial error of different estimation functions $\tilde{\lambda}^*$ is introduced as

$$\tilde{\varepsilon}^*(\mu) = \frac{\tilde{\lambda}^*(\mu, \lambda = 0) - \lambda_S(\mu)}{\lambda_S(\mu)}. \tag{50}$$

Respective results are plotted in Fig. 12. Except for $\lambda^{\diamond\diamond}(\lambda)$,

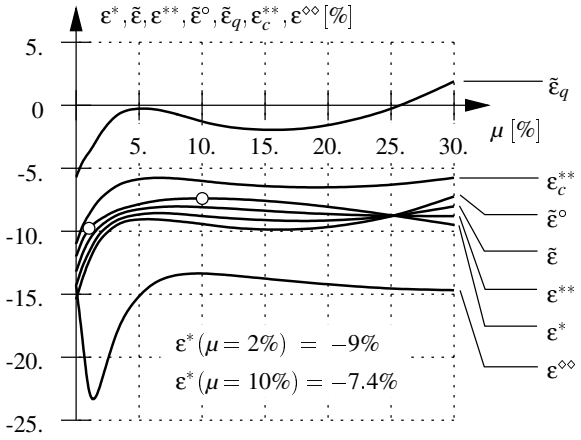

Figure 12 : Initial errors of different estimation functions over the dimensionless imperfection-parameter

the initial error of all estimation functions decreases with increasing degree of imperfection up to $\mu = 5\%$. For larger imperfections the initial estimation of λ_S based on λ^* does not strongly depend on μ. Nevertheless, especially the estimation function $\tilde{\lambda}_q$ yields estimates of λ_S which are sufficient reliable for structural design in the entire plotted range of μ.

4 Conclusions

Based on the angle between the eigenvector of the consistently linearized eigenvalue problem and the reference-load vector, a criterion for *ab initio* identification of the type of loss of stability can be derived. For the chosen parameterization, bifurcation and snap-through problems show different asymptotic properties. To obtain estimates of higher order, higher-order estimation functions, depending on the specific type of loss of stability, must be chosen. In parts of the prebuckling domain, where the higher-order estimation functions $\tilde{\lambda}$ and λ^{**} yield moderate errors, extensions of these higher-order estimation functions can further improve the reliability of the estimates which can be obtained. The order of such estimates is defined only in an asymptotic sense. Nevertheless, in general, highly reliable estimates are not only obtained in the so called *asymptotic domain*, i.e., in the immediate vicinity of λ_S, but also in an extended part of the entire prebuckling domain. For some problems, such as snap-through of the thicker perfect shell, even the initial estimates for λ_S are adequate for structural designing.

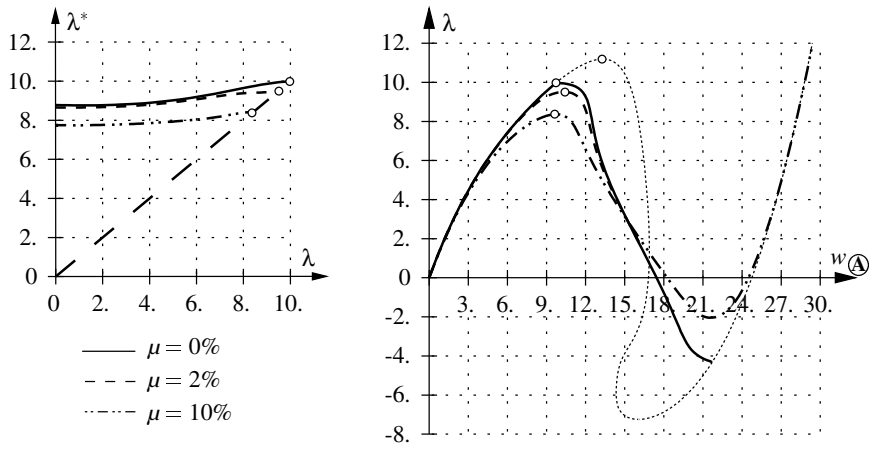

Figure 11 : Eigenvalue-curves and load-displacement diagrams for $\mu = 0\%$, $\mu = 2\%$, and $\mu = 10\%$

In case of bifurcation buckling with a strong influence of the nonlinearity in the prebuckling domain, as is the case for the thinner perfect shell, $\lambda^*(\lambda)$ may be a non-monotonic function. Nevertheless, the relative errors of λ^* do not exceed $\approx \pm 25\%$ as was shown in comprehensive numerical studies [Helnwein (1998)]. The constraint for bifurcation-modes, characterized by the validity of $\delta\mathbf{q}^{*T}\overline{\mathbf{P}} = 0$ in the *entire* prebuckling domain, may be the reason for this situation. A second consequence of the aforementioned constraint is that the rotations of the bifurcation-mode are significantly smaller than those concerning the snap-through mode.

The study of imperfect shells has shown, that also for the case of imperfection-sensitive structural behavior *ab initio* estimates of stability limits may be adequate for structural design.

References

Brendel, B. (1979): *Geometrisch nichtlineare Elastostatik*. Dr.-Ing. dissertation, University of Stuttgart, Germany, Institut for Statics, 1979. In German.

Brendel, B.; Ramm, E.; Fischer, F.; Rammerstorfer, F. (1981): Linear and nonlinear stability analysis of thin cylindrical shells under wind loads. *Structural Mechanics*, vol. 9, pp. 91–113.

Bushnell, D. (1972): Stress, stability and vibration of complex branched shells of revolution: Analysis and user manual for BOSOR 4. *NASA CR-2116*.

Gallagher, R.; Yang, H. (1968): Elastic instability predictions for doubly-curved shells. In *Proceedings of the 2nd Conference on Matrix Methods in Structural Mechanics*, pp. 711–739, Wright-Patterson A.F. Base, Ohio.

Helnwein, P. (1991): Begleitende lineare Eigenwertanalysen für Stabilitätsprobleme mit geometrisch nichtlinearem Vorbeulpfad – Eine numerische Untersuchung mittels der FEM. Dipl.-Ing.-thesis, Vienna University of Technology, 1991. In German.

Helnwein, P. (1998): *Zur initialen Abschätzbarkeit von Stabilitätsgrenzen auf nichtlinearen Last-Verschiebungspfaden elastischer Strukturen mittels der Methode der Finiten Elemente*, volume 79 of *Dissertationen an der Technischen Universität Wien*. Österreichischer Kunst- und Kulturverlag, Austria. In German.

Helnwein, P.; Mang, H. (1997): An asymptotic approach for the evaluation of errors resulting from estimations of stability limits in nonlinear elasticity. *Acta Mechanica*.

Helnwein, P.; Mang, H.; Pichler, B. (1999): Ab initio estimates of stability limits on nonlinear load-displacement paths: potential and limitations. *Computer Assisted Mechanics and Engineering Sciences*. In print.

Mallet, R.; Marçal, P. (1968): Finite element analysis of nonlinear structures. *J. Struct. Div. Proc. ASCE 94*, pp. 2081–2105.

Mang, H.; Helnwein, P. (1993): Lower and upper bounds for stability limits on geometrically nonlinear prebuckling paths. In Valliappan, S.; Pulmano, V.; Tin-Loi, F.(Eds): *Proceedings of the Second Asian-Pacific Conference on Computational Mechanics*, pp. 157–164, Sydney, Australien. Balkema, Rotterdam-Boston.

Mang, H.; Helnwein, P. (1995): A priori estimates of stability limits on nonlinear load-displacement paths. In Obrebski, J.(Ed): *Proceedings of the International Conference on Lightweight Structures in Civil Engineering*, volume II, pp. 811–821, Warschau, Polen. Magat Warschau.

Mang, H.; Helnwein, P. (1995): Second-order a-priori estimates of bifurcation points on geometrically nonlinear prebuckling paths. In Atluri, S.; Yagawa, G.; Cruse, T.(Eds):

Computational Mechanics '95. Proceedings of the International Conference of Computational Engineering Science, volume II, pp. 1511–1516, Hawaii, USA. Springer-Verlag, Berlin.

Mang, H.; Helnwein, P. (1999): Zur initialen Identifizierung von Verzweigungspunkten auf nichtlinearen Last-Verschiebungspfaden. *Zeitschrift für Angewandte Mathematik und Mechanik*. In print.

Pichler, B. (1999): Zur Zuverlässigkeit initialer Abschätzungen von Stabilitätsgrenzen auf nichtlinearen Last-Verschiebungspfaden elastischer Strukturen mittels der Methode der Finiten Elemente. Dipl.-Ing.-thesis, Vienna University of Technology, Austria, 1999. In German.

Sabir, A.; Lock, A. (1972): The application of finite elements to the large deflection geometrically nonlinear behaviour of cylindrical shells. In *Variational Methods in Engineering*, volume 7, pp. 66–75, Southhampton. University Press.

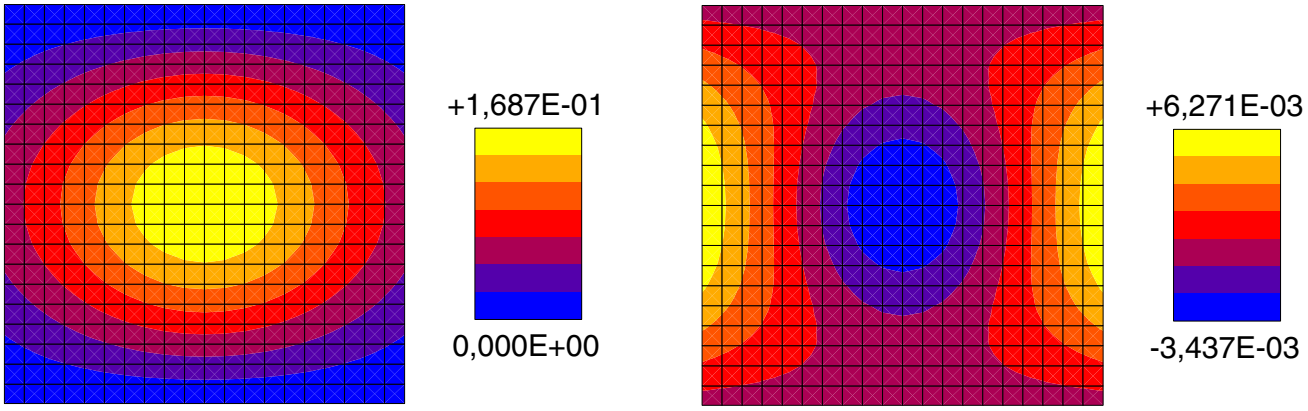

Figure 13 : $t = 12.7$cm, snap-through, component of $\delta\mathbf{q}^*$ (left plot) and $\delta\mathbf{q}^{*\prime}$ (right plot), in the vertical direction, at $\lambda = 0$

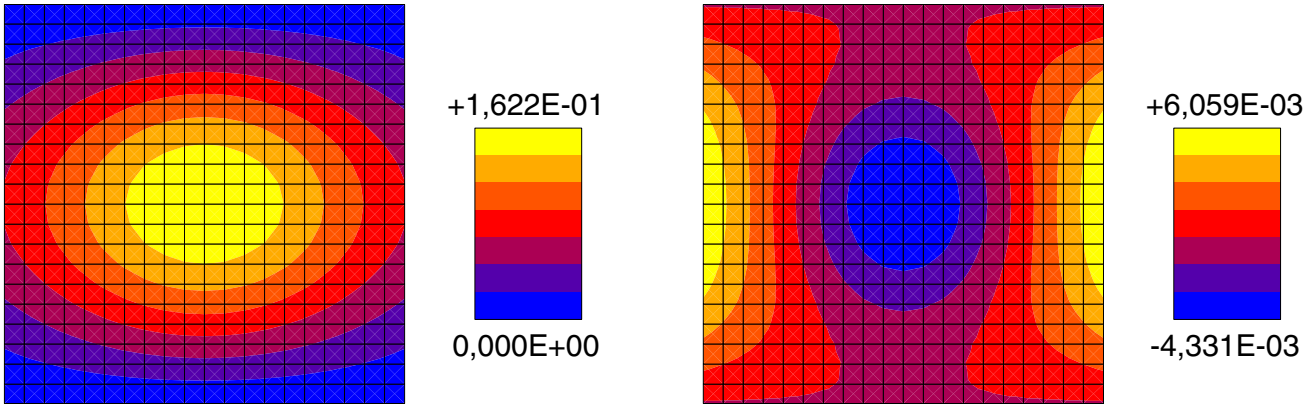

Figure 14 : $t = 12.7$cm, snap-through, component of $\delta\mathbf{q}^*$ (left plot) and $\delta\mathbf{q}^{*\prime}$ (right plot), in the vertical direction, at $\lambda = 1,70$ $\Rightarrow \Omega = 0$

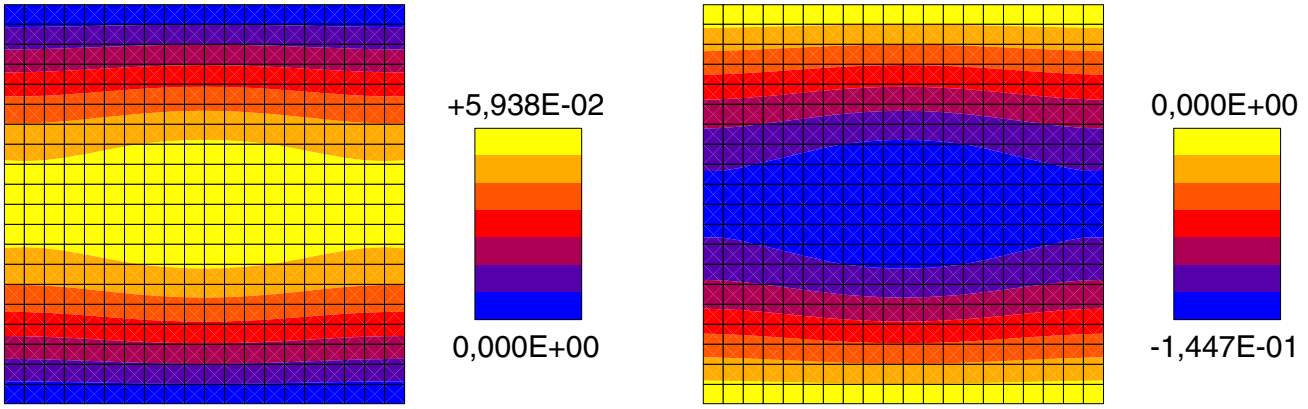

Figure 15 : $t = 12.7$cm, snap-through, component of $\delta\mathbf{q}^*$ (left plot) and $\delta\mathbf{q}^{*\prime}$ (right plot), in the vertical direction, at $\lambda = 9,90 = 0,99\,\lambda_S$

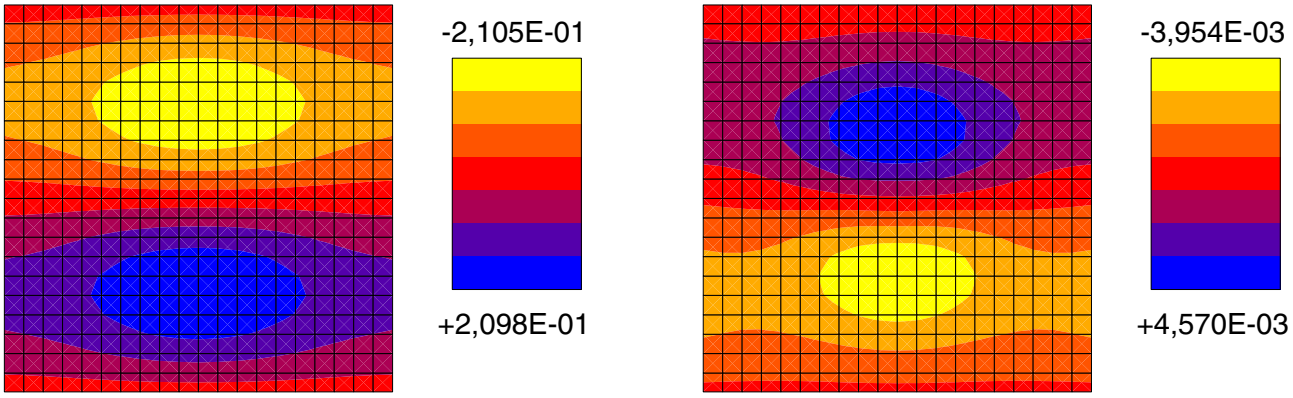

Figure 16 : $t = 6.35$cm, bifurcation, component of $\delta\mathbf{q}^*$ (left plot) and $\delta\mathbf{q}^{*\prime}$ (right plot), in the vertical direction, at $\lambda = 0$

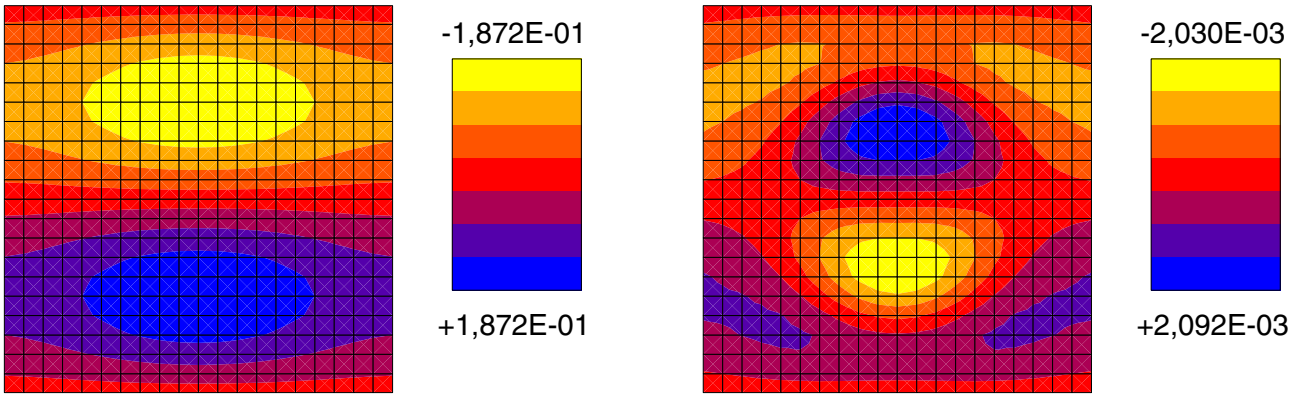

Figure 17 : $t = 6.35$cm, bifurcation, component of $\delta\mathbf{q}^*$ (left plot) and $\delta\mathbf{q}^{*\prime}$ (right plot), in the vertical direction, at $\lambda = 6,36 \Rightarrow \Omega = 0$

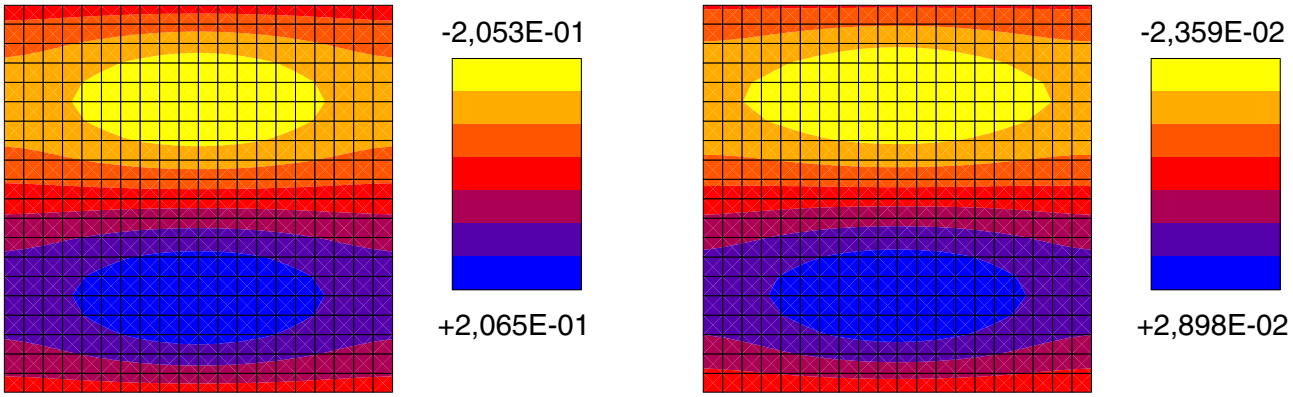

Figure 18 : $t = 6.35$cm, bifurcation, component of $\delta\mathbf{q}^*$ (left plot) and $\delta\mathbf{q}^{*\prime}$ (right plot), in the vertical direction, at $\lambda = 9,75 = 0.975\lambda_S$